ACS SENSORS

Article

Cite This: ACS Sens. 2018, 3, 2327−2334

pubs.acs.org/acssensors

Rapid Mouse Follicle Stimulating Hormone Quantification and Estrus Cycle Analysis Using an Automated Microfluidic Chemiluminescent ELISA System

Xiaotian Tan,[†] Anu David,[†] James Day,[†] Haoyue Tang,[‡] Emily Rose Dixon,[‡] Hongbo Zhu,[†] Yu-Cheng Chen,[†] Maung Kyaw Khaing Oo,*[,‡] Ariella Shikanov,*[,†] and Xudong Fan*[,†]

[†]Department of Biomedical Engineering, University of Michigan 1101 Beal Avenue, Ann Arbor, Michigan 48109, United States

[‡]Optofluidic Bioassay, LLC 600 South Wagner Street, Suite 131, Ann Arbor, Michigan 48103, United States

Supporting Information

ABSTRACT: Follicle stimulating hormone (FSH) plays a critical role in female reproductive development and homeostasis. The blood/serum concentration of FSH is an important marker for reporting multiple endocrinal functions. The standardized method for mouse FSH (mFSH) quantification based on radioimmunoassay (RIA) suffers from long assay time (~2 days), relatively low sensitivity, larger sample volume (60 μL), and small dynamic range (2−60 ng/mL); thus, it is insufficient for monitoring fast developing events with relatively small mFSH fluctuations (e.g., estrous cycles of mammals). Here, we developed an automated microfluidic chemiluminescent ELISA device along with the disposal sensor array and the corresponding detection protocol for rapid and quantitative analysis of mFSH from mouse tail serum samples. With this technology, highly sensitive quantification of mFSH can be accomplished within 30 min using only 8 μL of the serum sample. It is further shown that our technique is able to generate results comparable to RIA but has a significantly improved dynamic range that covers 0.5−250 ng/mL. The performance of this technology was evaluated with blood samples collected from ovariectomized animals and animals with reimplanted ovarian tissues, which restored ovarian endocrine function and correlated with estrus cycle analysis study.

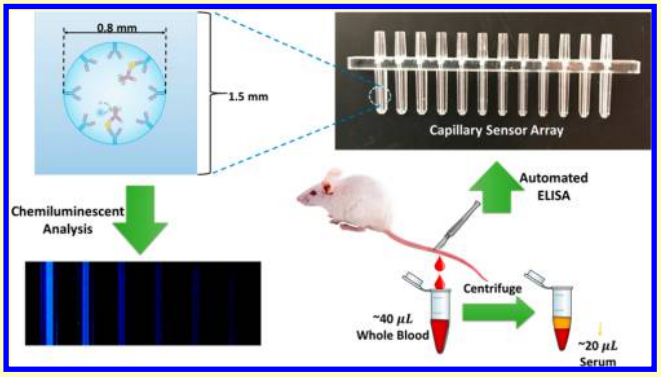

KEYWORDS: *microfluidics, ELISA, chemiluminescence detection, follicle stimulating hormone, estrus cycle analysis*

Follicle stimulating hormone (FSH) is one of the two gonadotropic hormones (along with luteinizing hormone, LH) that is released by the anterior lobe of the pituitary gland.[1] It plays a key role in female reproductive development and homeostasis through stimulating the maturation of germ cells and initiating follicular growth.[2,3] The blood/serum concentration of FSH is an important marker for reporting the function of the hypothalamic−pituitary−gonadal axis (HPG axis),[4,5] the stages of puberty and stages in estrus cycle in mammals, as well as the stages in the human menstruation cycle.[6] In each estrus cycle, the concentration of FSH in circulating blood can change dramatically in a very short period of time.[7,8] For rapidly monitoring the FSH concentrations in such events, a fast, reliable, sensitive, and on-site measurement with small sample consumption is highly desired.

The endocrine system of a mouse has been extensively studied for several decades and serves as one of the well-established model animals. The quantitative measurement of the serum FSH concentration is an important component of these studies. Currently, the blood/serum concentration of mouse FSH (mFSH) is most commonly quantified via radioimmunoassay (RIA). The antibody used in RIA (guinea pig polyclonal antibody in the form of antiserum) is designed for competitive immunoassay, thus having very good specificity. Consequently, RIA has been viewed as the "gold standard" for quantifying FSH concentration in serum.[9] However, the RIA assay for quantification of mFSH via RIA presents several challenges, such as relatively low sensitivity, large measurement uncertainty, and a small dynamic range (which varies over ~2−60 ng/mL) and requires 60 μL of sample for a single reading.[10] More importantly, the entire assay takes on the time-scale of days to complete. Such limitations make high power dilution of precious samples (such as mouse tail vein sera) unavoidable. Moreover, the high-power dilution will probably bring some samples (e.g., serum from mice that are in the estrus stage of the estrus cycles) out of their dynamic range. Because of these reasons, the RIA approach is insufficient for monitoring fast developing events with relatively small mFSH fluctuations, such as the estrous cycle of a mouse, especially in real- or quasi-real-time.

Received: July 12, 2018
Accepted: October 18, 2018
Published: October 18, 2018

DOI: 10.1021/acssensors.8b00641
ACS Sens. 2018, 3, 2327−2334

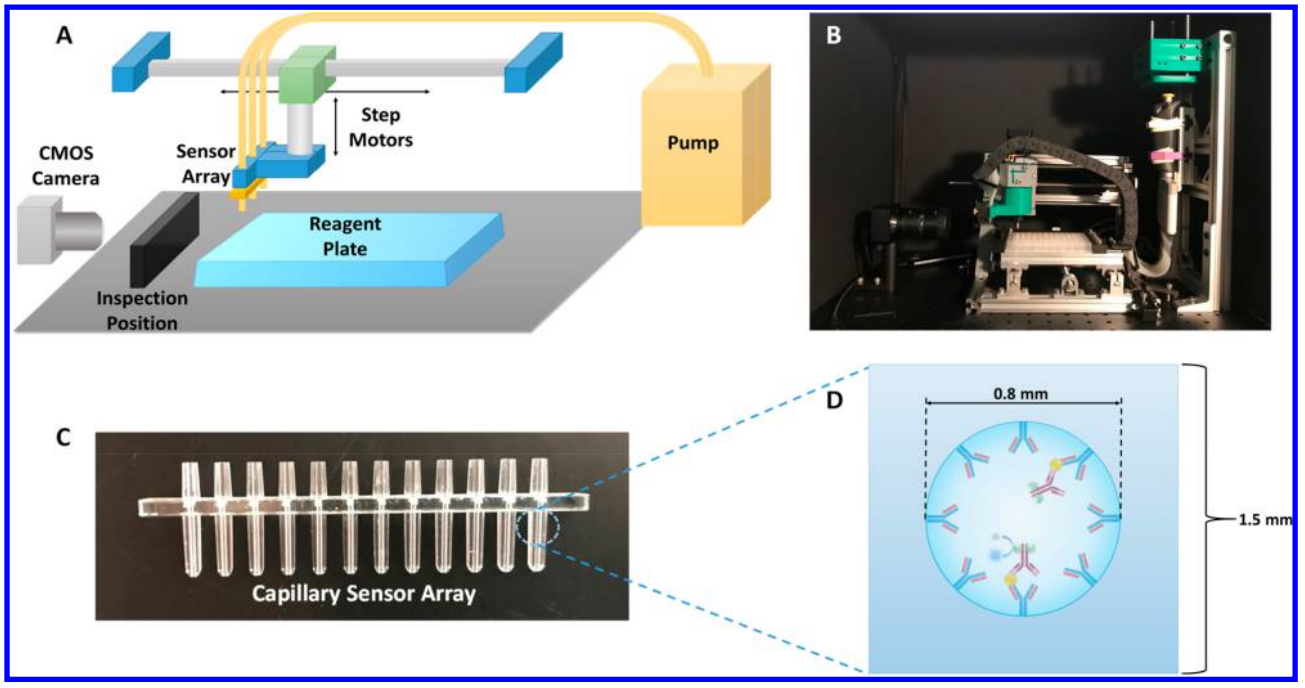

Figure 1. Layout, structure, and components of the automated ELISA device. (A) Illustration and (B) picture of the entire system. (C) Picture of a capillary sensor array. Each array contained 12 capillary units. The top portion of the array was connected to a liquid pump, and the bottom portion was used to withdraw samples/reagents stored in the regent plate. (D) Cross-sectional view of a capillary with an inner diameter of 0.8 mm and outer lateral size of 1.5 mm.

Enzyme-linked immunosorbent assay (ELISA), specifically sandwich ELISA, provides an alternative approach to RIA for FSH quantification. Benefiting from the use of antibody pairs, sandwich ELISA usually has high specificity toward target antigens. This technique indeed improves the efficiency of human FSH quantification (from 2 days to ~5 h).[11,12] However, because of the structural complexity, there is still no reliable commercial ELISA kit available for mFSH detection (most of the commercial kits could not generate results comparable to those obtained with the gold standard RIA method). Furthermore, ELISA using a traditional 96-well plate suffers from other technical drawbacks, such as large sample/reagent consumption (~100 μL) and relatively long assay time (~5 h).

In the past decade, various types of microfluidic ELISA devices have been developed to resolve the aforementioned problems of traditional ELISA.[13−18] However, most of them involve sophisticated fluidic designs and usually suffer from insufficient rinsing (due to residual liquids), low repeatability, strong background, small dynamic range, and large inter/intra-group variance.[14−17] In particular, no device or protocol exists for the rapid quantification of mFSH using small sample volumes. Here, we developed a fully automated and robust microfluidic chemiluminescent ELISA device, the disposable polystyrene capillary sensor array, and the corresponding assay protocol for rapid and quantitative analysis of mFSH from mouse tail sera. It is shown that the sensitive quantification of mFSH can be completed within 30 min using only 8 μL of serum sample. It is further shown that our method is able to generate results comparable to RIA but has a significantly improved dynamic range (0.5−250 ng/mL). Because of the simplicity of the capillary structure and automation, the results exhibited low background noise and small inter/intra-group variances. Finally, we applied the ELISA system in monitoring of the mFSH level across dramatic endocrine events, such as ovariectomy and transplantation of ovarian tissue, as well as moderate fluctuations during regular estrus cycles. Our work will lead to the development of an automated system that can be used for continuous monitoring and rapid analysis of mFSH and other analytes in research laboratories (especially for small animal research) and clinical settings.

MATERIALS AND METHODS

Automated ELISA System. *Instrument.* The automated ELISA system was designed, developed, assembled, and provided by Optofluidic Bioassay, LLC (Ann Arbor, MI) in collaboration with the University of Michigan. As illustrated in Figure 1, it consisted of a capillary sensor array, liquid pump, sample/reagent reservoir plate, digital CMOS camera, and robotic arms as well as control/communication modules and software.

Unlike conventional plate-based ELISA techniques that perform ELISA reactions in centimeter-scale reaction wells, our automated chemiluminescent ELISA was performed in polystyrene capillary sensor arrays. The sensor arrays (Figure 1C) were manufactured with the injection molding method. Each array contained 12 individual capillaries, each of which served as an ELISA reactor as well as a microfluidic channel. Benefitting from this industrial-grade fabrication technique, the sensor arrays have tight quality control, thus significantly improving inter/intra-assay variations. As shown in Figure 1D, the cross section of each capillary was designed to be circular to achieve better rinsing and avoid the potential liquid residuals at the channel corners. Each capillary had an inner diameter of 0.8 mm and total length of 16 mm. Therefore, the maximal ELISA reactor volume was only 8 μL. The capillary had a surface-to-volume ratio of 5 mm^{-1}, ~7-times higher than that for a traditional flat-bottom 96-well plate (0.73 mm^{-1}), which significantly increases the analyte capture efficiency and shortens the incubation time, as we demonstrated previously.[19]

The top portion of each capillary was connected to a liquid pump to control the liquid into and out of the capillary. As illustrated in Figure 1A, during the operation, the samples and reagents were first placed in the different wells on a reservoir plate (Thermo Fisher 384-

DOI: 10.1021/acssensors.8b00641
ACS Sens. 2018, 3, 2327−2334

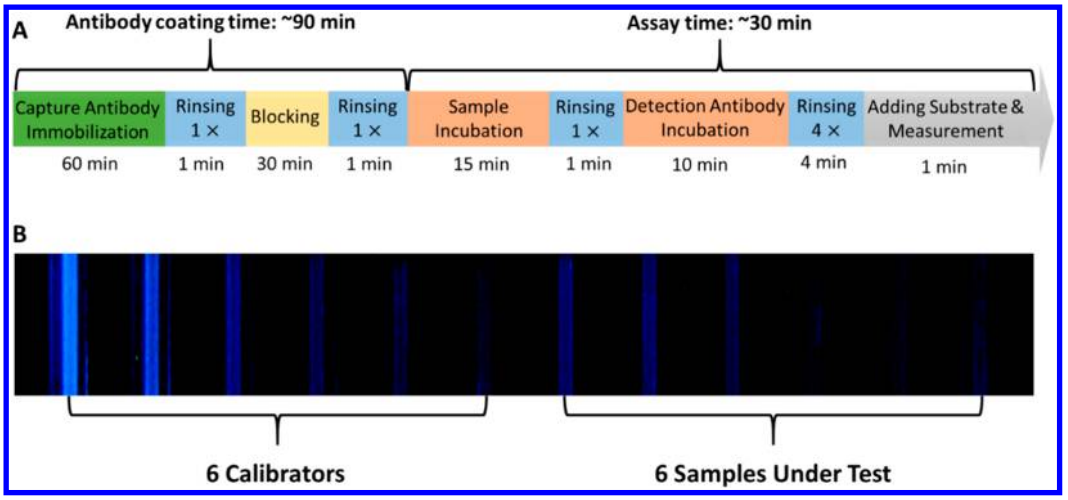

Figure 2. (A) Protocol for mouse FSH measurement with the automated ELISA system. (B) Capillary arrangement within a sensor array. Six capillaries on the left side were used as calibrators to generate a calibration curve. The remaining 6 capillaries were used for measuring actual samples.

well plate, part no. 12-566-213). Robotic arms moved the sensor array to the corresponding wells and sequentially withdrew samples/reagents from the wells into the capillaries, incubated, and then ejected the wastes out of the capillaries. Finally, the sensor array was placed in front of a CMOS camera, and the chemiluminescence signal from each capillary was recorded for postexperiment analysis. The details of the operation for mFSH detection is presented later in the section Procedures of mFSH Analysis.

Chemical Reagents. The chemiluminescent substrate (SuperSignal ELISA Femto Substrate) was purchased from Thermo Fisher. The substrate kit (product no. 37075) contains a bottle of 50 mL Luminol + Enhancer Solution and a bottle of 50 mL Stable Peroxide Solution. The working substrate solution was prepared by equal-volumetric mixing of the Luminol + Enhancer Solution and the Stable Peroxide Solution at room temperature. The ELISA coating buffer (1× PBS, DY006), concentrated wash buffer (WA126), and concentrated reagent diluent (10% BSA in 10× PBS, DY995) were purchased from R&D Systems.

The mFSH standard used in this experiment was purchased from the National Hormone and Peptide Program (NHPP, AFP5308D). A mouse monoclonal antibody purchased from Thermo Fisher (P4G2, MIF2709) was used as the capture antibody. The detection antibody was purified from National Hormone and Peptide Program's guinea pig anti-mFSH antiserum (AFP-1760191). The detailed purification process can be found in the Supporting Information. Because the purified detection antibody did not come with any reporter enzyme, it was modified by conjugating with horseradish peroxidase (HRP) in a 1:4 molar ratio of antibody/HRP. The conjugation reaction was carried out with Abcam's HRP conjugation kit (ab102890).

The working solution of the wash buffer and reagent diluent were diluted with Milli-Q water (R = 18.2 Ω) to achieve 1× working concentration. For simulating the properties (e.g., viscosity) of actual mouse serum, the antigen solvent, as well as the blocking buffer, used in this experiment were prepared by mixing fetal bovine serum (FBS) and 1× reagent diluent (1% BSA in PBS) in a volumetric ratio of 1:1.

The working solution of the capture antibody was prepared by diluting the stock solution with PBS buffer (pH 7.4) to achieve a final concentration of 12 μg/mL. The concentrated mFSH standard was diluted to a desired concentration with the premixed antigen solvent (i.e., 0.5× FBS). The working solution of the detection antibody was prepared by diluting the HRP-labeled detection antibody 400-times (with 1× reagent diluent) to its final working concentration.

Procedures of mFSH Analysis. All experiments were performed at the University of Michigan, Ann Arbor. An illustration of the entire assay (from blood collection to final optical measurement) can be found in Figure S1. In each test, 6 capillaries were used as calibration references to generate a calibration curve. The remaining 6 capillaries were dedicated to samples under test. Depending on the number of samples, single, duplicate, and triplicate measurements could be performed on each sample.

Before starting a test, all reagents and samples were added to the corresponding wells on the reagent reservoir plate (Thermo Fisher square well 384-well plate, part number 12-566-213). For making the liquid easily accessible by the capillaries, 30 μL of reagents/samples were added to each well, although less than 10 μL of reagents/samples were needed for each well (and each capillary sensor). Because each capillary sensor needed only ∼8 μL of reagents/samples in each test, the remaining volume (∼22 μL) can be collected and reused in further experiments. In the near future, customized reagent reservoir plates will be used to accommodate the capillary sensor array so that only ∼10 μL for sample/reagent is needed to fill each well in the reservoir plate.

The capillary sensors needed to go through capture antibody coating and surface blocking before actual sample measurement (see Figure 2A). The capture antibody immobilization (through physical adsorption) was performed by incubating the capture antibody working solution at room temperature in the capillary for 1 h. After rinsing with wash buffer, the blocking buffer was added and incubated for another 30 min.

The actual assay included three steps, sample incubation, detection antibody incubation, and chemiluminescent intensity measurement, as illustrated in Figure 2A. The sample incubation and detection antibody incubation took 15 and 10 min, respectively. The chemiluminescent intensity measurement was performed immediately after adding the substrate to the capillary reactors. (According to the user's manual, the emission intensity of the SuperSignal substrate remains steady for first few minutes of incubation.) The total assay time was ∼30 min, including ∼5 min of rinsing, the time for robotic arm movements, and optical detection, which is ∼100-times faster than the standard mFSH RIA test (which usually takes ∼2 days[10,20]), 10-times faster than a typical sandwich ELISA assay (for example, according to the user's manual of a typical sandwich ELISA kit from R&D Systems, the total assay time is ∼320 min), and similar to most of the microfluidic ELISA techniques designed for protein quantification.[14,17,21]

The results of the capillary chemiluminescent ELISA experiments were recorded with a CMOS camera and subsequently quantified through a previously established chemiluminescent imaging method.[19] Briefly speaking, signal from the blue channel was extracted from the image. Then, the intensity along the central axis of each capillary was recorded and then averaged along the capillary longitudinal direction with ImageJ software. More details can be found in our previous work.[19]

DOI: 10.1021/acssensors.8b00641
ACS Sens. 2018, 3, 2327−2334

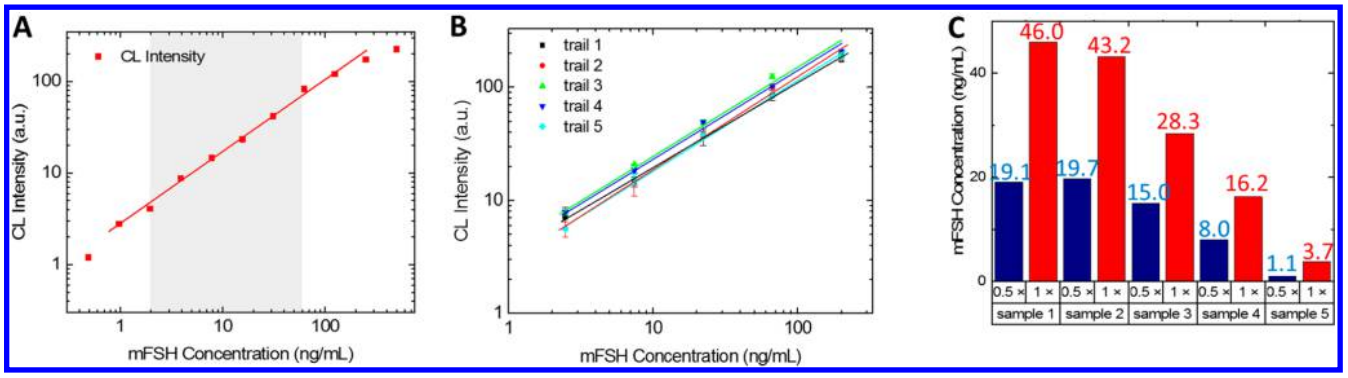

Figure 3. Calibration results of the mFSH assay. (A) Dynamic range of the FSH assay. The linear response range is between 1 and 250 ng/mL. The red line is the linear regression between 1 and 250 ng/mL in the log−log scale. The shaded area denotes the dynamic range of mFSH RIA. (B) Intergroup performance of the automated ELISA system for the mFSH assay. The intergroup variances at 200, 66.67, 22.22, 7.41, and 2.47 ng/mL are 1.27, 3.50, 3.93, 5.80, and 9.08%, respectively. The error bars are the standard deviations calculated from duplicate measurements. The solid lines are linear regressions in the log−log scale. (C) Measurement results before and after 2× dilution.

Animal Experiments. *Ethics.* The IACUC guidelines for survival surgery in rodents and the IACUC Policy on Analgesic Use in Animals Undergoing Surgery were followed for all of the procedures (PRO00007716).

Blood Collection. In each collection, ∼40 μL of blood was collected from the lateral tail vein at designated time points with a 53/4 in. glass Pasteur pipet up to the time of sacrifice. After collection, all samples were stored at 4 °C overnight and centrifuged for 10 min at 10,000 rpm, and the collected serum was stored at −20 °C.

Vaginal Cytology for Estrus Cycle Evaluation. For the estrus cycle to be assessed, vaginal cytology was performed in mice. Vaginal cytology was resumed after 7 days following all procedures (ovariectomies and subcutaneous implantations of ovarian tissue) and was performed daily until sacrifice. The transition from leukocytes to cornified cells at least once a week was considered as a resumed or continued cycle.

Histological Analysis of Retrieved Ovaries. Following sacrifice, the implanted ovaries were retrieved from mice and fixed in Bouin's fixative at 4 °C overnight. The fixed ovaries were then transferred and stored in 70% ethanol at 4 °C. After processing, samples were embedded in paraffin, serially sectioned at 5 μm thickness, and stained with hematoxylin and eosin.

RESULTS

Assay Performance Evaluation. The calibration measurement results using the mFSH standards (500, 250, 125, 62.5, 31.25, 15.63, 7.81, 3.91, 1.95, 0.98, 0.49, and 0 ng/mL) with the automated ELISA system are shown in Figure 3A. The data point at 0 ng/mL serves as the background of the assay and is subtracted from the readings of other concentrations. The linear dynamic range of the mFSH assay is between 1 and 250 ng/mL, which is significantly broader than the dynamic range in conventional RIA (shown as the shaded area in Figure 3A). The limit of detection is 0.5 ng/mL. The calibration curve (between 1 and 250 ng/mL) has a slope of 0.77 in the log−log scale. Because the detection antibody used in our work is the same as the one used in conventional RIA,[10,20] our technique should have the same or improved specificity due to the employment of the additional monoclonal capture antibody.[22] A comparison between the RIA's calibration curve (dynamic range varying between 1.6 and 37 ng/mL and 3−75 ng/mL) and the calibration curve obtained with our ELISA system can be found in Figure S2.

In practice, 6 capillaries were used for calibrators, and the other 6 capillaries were for actual samples. Therefore, we selected five different mFSH concentrations within the linear response range in Figure 3A (200, 66.67, 22.22, 7.41, and 2.47 ng/mL) as well as a zero background (50% FBS in 1% BSA) to generate the calibration curve. For the intergroup consistency of our ELISA system to be analyzed, multiple mFSH assays with these calibration concentrations were performed on different days. The results are presented in Figure 3B. The background reading was subtracted from those of nonzero mFSH concentrations. The slopes of these five calibration curves were very close to each other. The average slope (in the log−log scale) was 0.77, and the standard deviation for the slopes was 0.03. The intergroup variances at 200, 66.67, 22.22, 7.41, and 2.47 ng/mL are 1.27, 3.50, 3.93, 5.80, and 9.08%, respectively. These data indicate the stability of our system is better than mFSH RIA (see SI Figure 2) and on par with (or even better than) most of the conventional ELISA techniques[23] and competing microfluidic ELISA devices.[17,24,25]

Because the amount of serum is limited and usually less than our desired volume (30 μL), 2-times dilution became necessary for most of the samples. To explore the impact on measurements caused by dilution, we performed a comparison experiment on five samples. As the results show in Figure 3C, the measurement results obtained with 2-times diluted samples were close to 0.5-times of the results generated with original serum. These results indicate that the dilution does not cause significant errors that affect further analysis. In the future, a smaller reservoir plate will be used with only ∼10 μL for each well so that dilution of serum samples will become unnecessary. In addition, the measurement results generated with our microfluidic chemiluminescent ELISA are generally comparable to those generated with RIA (as presented in Figure S3).

Tracking mFSH Level in Postovariectomized Mice. To verify the practicality of this technique in real-world animal research, we designed a long-term study for tracking the mFSH level in mouse serum over dramatic endocrine events using a group of healthy wild type mice (n = 4). Briefly, on day 0 of this study, we performed ovariectomy (removal of ovaries) in all four mice within this group. On day 35 of this study, we transplanted a functional ovary into two of the four mice. To reduce the organ rejection effect, we collected the ovaries from two donors that have the same genotype with the experiment subject.[26,27] All four mice were sacrificed on day 98, which corresponds to the end of this study. As described in the Materials and Methods, to closely monitor the blood mFSH

DOI: 10.1021/acssensors.8b00641
ACS Sens. 2018, 3, 2327−2334

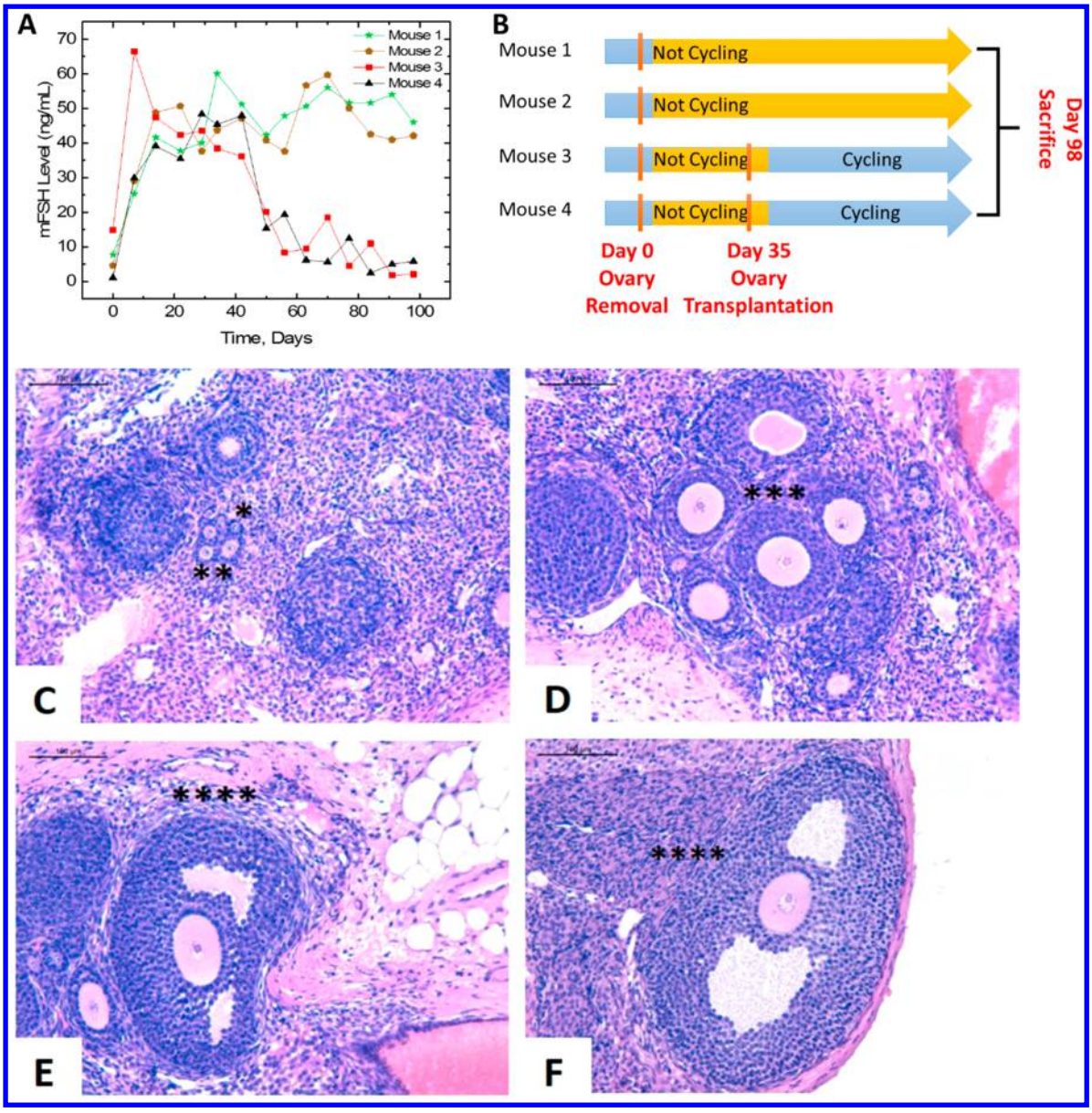

Figure 4. Surgery-related mFSH results. (A) mFSH measurement results for mice 1−4. The ovariectomy surgeries were performed on day 0 (for all four mice), and ovary implantation surgeries were performed on day 35 (for mice 3 and 4). (B) Qualitative summary of vaginal cytology results. Mice 3 and 4 started to cycle again after day 44 (9 days after ovary transplantation). (C−F) Histological images of syngeneic ovarian tissue subcutaneously implanted in ovariectomized mice showing (C) primordial (*) and primary follicles (**), (D) secondary follicles (***), and (E, F) antral follicles (****), which indicates the implanted ovaries were still functioning normally by day 98 (in mice 3 and 4); 20× magnification.

level without overly interfering with the animal's regular physiological function, ~40 μL of blood was collected from the tail vein of each mouse every 7 days, which means that ~20 μL of serum could be obtained after centrifugation.

Ovaries are hormone-secreting organs, and their removal causes a dramatic decrease in serum estrogen concentration (estrogen serves as a signaling molecule for the negative feedback), thus terminating the feedback control loop (hypothalamus-pituitary-gonadal axis) for mFSH stabilization. As a result, the anterior pituitary releases more mFSH to stimulate the ovaries that are not there to respond. Without the negative feedback of estradiol, the pituitary continues to release mFSH, resulting in increasing blood levels of the unregulated gonadotrophic factor.[28] For the effects of ovariectomy to be reversed, the ovary transplantation surgery restores the estrogen production and elevates concentrations in circulating blood. The restored feedback control system eventually lowers the mFSH concentration back to the normal range through restoration of the hypothalamus-pituitary-gonadal axis. If our methodology and device are sensitive enough, we should be able to observe the fluctuations in mFSH concentration that are directly related to these two surgical events (i.e., removal and transplantation of ovary).

As shown in Figure 4, the serum mFSH concentration for all four mice increased dramatically to >35 ng/mL within 2 weeks after ovariectomy. Starting from day 21 postovariectomy, the serum mFSH level of all four mice became steady at ~40 ng/mL, which indicates that the anterior pituitary glands reach their maximal mFSH productivity. On day 35, ovary transplantation surgeries were performed on mice 3 and 4. However, the mFSH level 1 week post-transplantation (day 42) remains mostly unchanged, indicating that the restoration

DOI: 10.1021/acssensors.8b00641
ACS Sens. 2018, 3, 2327−2334

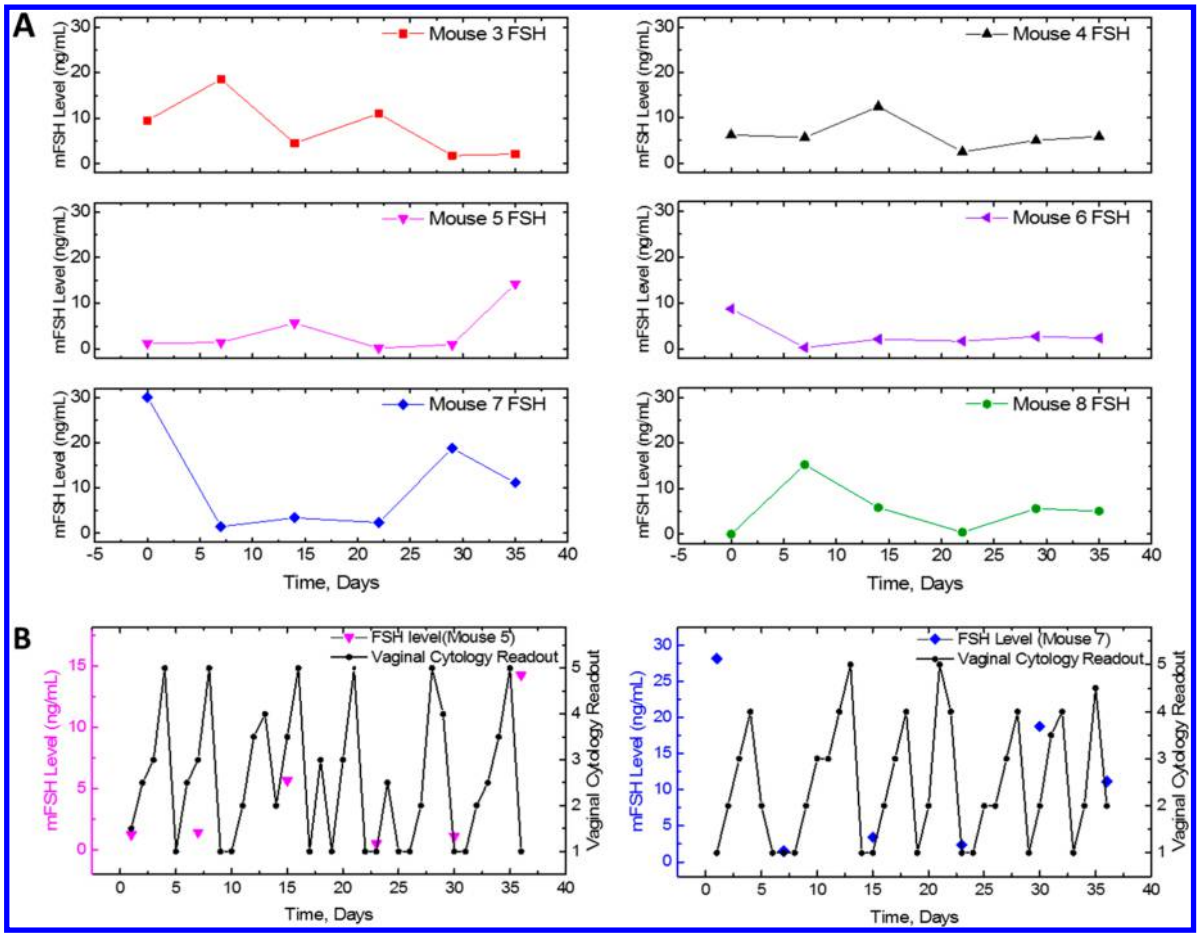

Figure 5. Estrus cycle analysis results. (A) mFSH measurements for six individual mice during a 36 day monitoring period. Clear fluctuations can be observed in all of them. The peak mFSH levels vary significantly among mice, whereas the valley mFSH levels remain quite similar. (B) Comparison between the cyclicity observed from vaginal cytology and mFSH measurements for mice 5 and 7. Both sets of comparisons show that the mFSH measurement lags the vaginal cytology readouts by 1−1.5 days.

of the feedback control loop takes more than 1 week to complete, which is consistent with other reports.[29,30] After that, the mFSH level in the two implanted mice started to drop back to the normal physiological range (<20 ng/mL). This significant decrease occurred between days 42 and 63. At 4 weeks post-transplantation, the mFSH level in mice 3 and 4 became mostly steady (averaged mFSH concentration < 10 ng/mL) with an obvious periodic fluctuation. In contrast, the mFSH level for mice 1 and 2 remained above 35 ng/mL. This phenomenon suggests that the implanted ovary tissue had successfully restored the estrus cycle in mice 3 and 4. As presented in Figure 4B, the restoration of the hypothalamus-pituitary-gonadal axis (shown as cellular cyclicity) for the ovary-implanted mice has been verified through vaginal cytology during the monitoring period. Histological analysis of the implanted ovaries (Figure 4C−F) correlated with our FSH serum levels and vaginal cytology measurements. Presence of postovulatory structures in the implanted ovarian tissue was confirmed by the presence of estrous cycles identified using vaginal cytology. In addition, there are still multiple early stage follicles in the transplanted ovary by the day of sacrifice (day 98). These pieces of evidence indicate that the implanted ovaries were still functioning by day 98. The results also proved that mice 3 and 4 could be deemed as heathy adult mice after day 63 of this study.

The results presented in Figure 4A clearly demonstrate the capability of our microfluidic chemiluminescent ELISA device to quantitatively differentiate the mFSH level before and after ovariectomy surgery as well as the change caused by ovary transplantation with only 20 μL of mouse tail serum. More importantly, the periodic fluctuation that we observed in the ovary-transplanted mice indicates that our technique can possibly differentiate the stages in a mouse's estrus cycle that usually has low mFSH levels (1−20 ng/mL).

Tracking mFSH Level over Estrus Cycles. To verify the ability of our ELISA system to quantitatively differentiate the stages in a mouse's estrus cycle through serum mFSH concentration, we designed another midterm in vivo study. Because mice have a very small total blood volume (~2.5 mL), we were unable to collect 40 μL of blood on a daily basis. Previous research has shown that the duration of an estrus cycle in mice is ~4−5 days and that the duration of one stage in a single cycle is ~1 day. Therefore, if we collect blood every 7 days, the collected serum samples will fall into different stages for at least every three collections. To verify this claim, we performed a five-week-long tail vein blood study with six healthy female mice (including the two ovary transplanted mice after day 63, mice 3 and 4).

Significant mFSH fluctuations in all mice in the study corresponded with the expected outcomes (Figure 5A). For each individual mouse, the difference between the peak mFSH

DOI: 10.1021/acssensors.8b00641
ACS Sens. 2018, 3, 2327−2334

and the valley mFSH values can be easily distinguished, suggesting that our technology is able to differentiate stages in an estrus cycle through mFSH concentrations. It is seen that the peak mFSH concentration varies significantly among all mice and falls into a wide range between 6 and 28 ng/mL. The valley mFSH concentration, however, is quite similar for all six mice, between 0.5 and 2.5 ng/mL.

The results collected with the mFSH chemiluminescent ELISA measurement were also compared with those obtained with daily vaginal cytology. Because the vaginal epithelial condition is directly regulated by the estrogen level, from vaginal cytology readouts we are able to estimate the corresponding estrogen level at that time point. To intuitively compare the vaginal cytology results and FSH measurements, we assigned numerical values to each stage in a vaginal epithelial cycle.[31,32] For example, the value for C phase (later estrus stage) was assigned to be 1, and the value for NLNC phase (later diestrus stage and early proestrus stage) was assigned to be 5 because the estrogen level usually reaches its peak level in this phase. Beside these two, CLNC, L, and LN phases were assigned to be 2−4, respectively. The intermediate situations were assigned to be the average between two neighboring stages (such as 2.5 and 3.5, etc.). The rule for assigning numerical values and the exemplary vaginal cytology readouts are shown in Figure S4.

With these numerical values, we can directly compare the vaginal cytology readouts and mFSH readout on the same plot. Mice 5 and 7 were selected as two representatives because they have the most obvious and stable cycling pattern. The results are shown in Figure 5B. The readouts from these two mice during the 35 days of experiment presented a lagging period between the vaginal cytology pattern and the measured mFSH pattern. On the basis of the results generated from these two mice, the lagging time is estimated to be ∼1 day, which agrees well with the pattern reported in the literature.[32−34]

DISCUSSION

In the mouse experiments, we observed a few interesting phenomena. For the ovary transplantation experiment, based on vaginal cytology measurements, the estrus cycle started to appear 9 days after implantation (day 44 from the start date of the study) and the serum mFSH concentration started to decrease on day 14 after implantation. This agrees with the theory that serum mFSH is a downstream marker during the restoration of the sex hormone feedback loop (hypothalamus-pituitary-gonadal axis). Previous research using the RIA-based mFSH quantification technique also observed the same phenomena (REF). However, because the required blood volume was relatively large (∼90 μL) and the time interval between two consecutive blood collections had to be 14 days for the well-being of the animals, it was difficult to quantify the lagging time between the restoration of gonad endocrine function and restoration of the feedback loop.[29,35] With the described ELISA system, we were able to shorten this time interval down to 1 week (with only ∼40 μL of blood). On the basis of the results shown in Figure 4A and B, we can see clearly that the delay between vaginal epithelial response (gonad endocrine function) and serum mFSH response (restoration of feedback loop) should be between 1 and 5 days. More accurate results can be generated if we can further reduce the time interval between two blood collections, which will also be our research direction in the near future.

In the estrus cycle study, we observed a very stable 1−1.5 days of lagging between the vaginal cytology readouts and serum mFSH readouts, which agrees with other researchers' opinions regarding interhormone correlation in mice estrus cycle.[33] However, previous studies show that the peak mFSH level is hard to capture because it only lasts for a short period of time (∼12 h).[36] On the basis of our current work, we can either predict the mFSH level from the noninvasive vaginal cytology readout or capture and quantify the mFSH peak intensity timely in each estrus cycle. Such capability is very beneficial to pituitary function and activity studies.

CONCLUSIONS

In this work, we have developed a robust and automated ELISA system and the corresponding protocol for mFSH measurement in which the mFSH measurement can be completed within 30 min by using 8 μL of serum sample (∼100-times faster and 7-times lesser of samples than RIA). Benefitting from the programmable automated operation, the inter-assay variance could reduce to <10%, thus achieving comparable results with RIA but having a significantly larger dynamic range (1−250 ng/mL), which is very beneficial for analyzing samples under extreme conditions, such as sera from postovariectomized mice and regular mice in the estrus/metestrus stages of their estrus cycles. The results presented in this work reveal that our technology has the ability to quantitatively differentiate the mFSH level before and after overiectomy surgery as well as the changes caused by ovary transplantation surgery. In addition, our technology is able to differentiate stages in an estrus cycle, even at low mFSH levels (1−20 ng/mL). More significantly, the dynamic range is adjustable through changing the incubation times, which resulted in a detection limit as low as 0.25 ng/mL. Such a feature can certainly benefit studies for different purposes, especially for monitoring estrus cycles with a high sampling frequency. Because the concept of this assay (sandwich immunoassay) is universal, it can easily be adapted for the quantification of any other proteins, hormones, and peptides (the only limitation is the availability of antibodies). In the near future, we envision that this system may have the capability to monitor various types of specific functional proteins in precious animal samples (e.g., urine, saliva, or even whole blood) besides the mFSH levels in mouse serum. Owing to the compact size of the commercial plate reader, the device can be exploited for on-site detection. By reengineering the design of the reagent reservoir plate, the required sample volume is expected to be further reduced to ∼10 μL, providing a much more efficient paradigm for quantification and biomedical analysis.

ASSOCIATED CONTENT

Supporting Information

The Supporting Information is available free of charge on the ACS Publications website at DOI: 10.1021/acssensors.8b00641.

Illustration for the procedure of the entire mFSH assay, comparison of the dynamic range between the mFSH RIA and our instrument/method, comparison between the readings measured with our ELISA system and traditional RIA, and the rules for assigning values to different stages in an estrus cycle (PDF)

DOI: 10.1021/acssensors.8b00641
ACS Sens. 2018, 3, 2327−2334

AUTHOR INFORMATION

Corresponding Authors

*E-mail: maungk@optobio.com.
*E-mail: shikanov@umich.edu.
*E-mail: xsfan@umich.edu.

ORCID

Xudong Fan: 0000-0003-0149-1326

Notes

The authors declare the following competing financial interest(s): M.K.K.O. and X.F. are co-founders of and have an equity interest in Optofluidic Bioassay, LLC.

ACKNOWLEDGMENTS

The authors thank Dr. A. F. Parlow for providing mouse FSH standards and antisera. This research was supported by National Science Foundation (DBI-1451127), National Institutes of Health R01 EB022033, and National Science Foundation Graduate Research Fellowship (DGE 1256260).

REFERENCES

(1) Pierce, J. G.; Parsons, T. F. Glycoprotein hormones: structure and function. *Annu. Rev. Biochem.* **1981**, *50* (1), 465−495.

(2) Le Tissier, P.; Hodson, D.; Lafont, C.; Fontanaud, P.; Schaeffer, M.; Mollard, P. Anterior pituitary cell networks. *Front. Neuroendocrinol.* **2012**, *33* (3), 252−266.

(3) Jiang, X.; Liu, H.; Chen, X.; Chen, P.-H.; Fischer, D.; Sriraman, V.; Yu, H. N.; Arkinstall, S.; He, X. Structure of follicle-stimulating hormone in complex with the entire ectodomain of its receptor. *Proc. Natl. Acad. Sci. U. S. A.* **2012**, *109* (31), 12491−12496.

(4) Meethal, S. V.; Atwood, C. The role of hypothalamic-pituitary-gonadal hormones in the normal structure and functioning of the brain. *Cell. Mol. Life Sci.* **2005**, *62* (3), 257−270.

(5) Marieb, E. N.; Hoehn, K. *Human anatomy & physiology*; Pearson Education, 2007.

(6) Nelson, R. J. *An introduction to behavioral endocrinology*; Sinauer Associates, 2011.

(7) Butcher, R.; Collins, W.; Fugo, N. Plasma concentration of LH, FSH, prolactin, progesterone and estradiol-17β throughout the 4-day estrous cycle of the rat. *Endocrinology* **1974**, *94* (6), 1704−1708.

(8) Sherman, B. M.; Korenman, S. G. Measurement of serum LH, FSH, estradiol and progesterone in disorders of the human menstrual cycle: the inadequate luteal phase. *J. Clin. Endocrinol. Metab.* **1974**, *39* (1), 145−149.

(9) Pratt, J.; Woldring, M. Radioimmunoassay specificity and the "first-come, first-served effect. *Clin. Chim. Acta* **1976**, *68* (1), 87−90.

(10) University of Virginia School of Medicine Assay Methods. https://med.virginia.edu/research-in-reproduction/ligand-assay-analysis-core/assay-methods/ (accessed 09/14/2018).

(11) Liew, M.; Groll, M. C.; Thompson, J. E.; Call, S. L.; Moser, J. E.; Hoopes, J. D.; Voelkerding, K.; Wittwer, C.; Spendlove, R. S. Validating a custom multiplex ELISA against individual commercial immunoassays using clinical samples. *BioTechniques* **2007**, *42* (3), 327−328.

(12) Lindau-Shepard, B.; Roth, K. E.; Dias, J. A. Identification of amino acids in the C-terminal region of human follicle-stimulating hormone (FSH) beta-subunit involved in binding to human FSH receptor. *Endocrinology* **1994**, *135* (3), 1235−1240.

(13) Madaboosi, N.; Pedrosa, C. R.; Reis, M. F.; Soares, R. R.; Chu, V.; Conde, J. P. In *Microfluidic ELISA for sensing of prostate cancer biomarkers using integrated a-Si: H pin photodiodes*, Sensors, 2014 IEEE, 2014; pp 881−884.

(14) Giri, B.; Dutta, D. Improvement in the sensitivity of microfluidic ELISA through field amplified stacking of the enzyme reaction product. *Anal. Chim. Acta* **2014**, *810*, 32−38.

(15) Hoegger, D.; Morier, P.; Vollet, C.; Heini, D.; Reymond, F.; Rossier, J. S. Disposable microfluidic ELISA for the rapid determination of folic acid content in food products. *Anal. Bioanal. Chem.* **2006**, *387* (1), 267−275.

(16) Herrmann, M.; Veres, T.; Tabrizian, M. Enzymatically-generated fluorescent detection in micro-channels with internal magnetic mixing for the development of parallel microfluidic ELISA. *Lab Chip* **2006**, *6* (4), 555−560.

(17) Kubo, I.; Kanamatsu, T.; Furutani, S. Microfluidic Device for Enzyme-Linked Immunosorbent Assay (ELISA) and Its Application to Bisphenol A Sensing. *Sens. Mater.* **2014**, *26* (8), 615−621.

(18) Proczek, G.; Gassner, A.-L.; Busnel, J.-M.; Girault, H. H. Total serum IgE quantification by microfluidic ELISA using magnetic beads. *Anal. Bioanal. Chem.* **2012**, *402* (8), 2645−2653.

(19) Tan, X.; Khaing Oo, M. K.; Gong, Y.; Li, Y.; Zhu, H.; Fan, X. Glass capillary based microfluidic ELISA for rapid diagnostics. *Analyst* **2017**, *142*, 2378−2385.

(20) University of Wisconsin WNPRC Assay Service Home. https://www.primate.wisc.edu/?page_id=2231 (accessed 09/14/2018).

(21) Mirasoli, M.; Guardigli, M.; Michelini, E.; Roda, A. Recent advancements in chemical luminescence-based lab-on-chip and microfluidic platforms for bioanalysis. *J. Pharm. Biomed. Anal.* **2014**, *87*, 36−52.

(22) Pei, X.; Zhang, B.; Tang, J.; Liu, B.; Lai, W.; Tang, D. Sandwich-type immunosensors and immunoassays exploiting nanostructure labels: A review. *Anal. Chim. Acta* **2013**, *758*, 1−18.

(23) Baines, H.; Nwagwu, M. O.; Hastie, G. R.; Wiles, R. A.; Mayhew, T. M.; Ebling, F. J. Effects of estradiol and FSH on maturation of the testis in the hypogonadal (hpg) mouse. *Reprod. Biol. Endocrinol.* **2008**, *6* (1), 4.

(24) Otieno, B. A.; Krause, C. E.; Jones, A. L.; Kremer, R. B.; Rusling, J. F. Cancer diagnostics via ultrasensitive multiplexed detection of parathyroid hormone-related peptides with a microfluidic immunoarray. *Anal. Chem.* **2016**, *88* (18), 9269−9275.

(25) Novo, P.; Chu, V.; Conde, J. Integrated optical detection of autonomous capillary microfluidic immunoassays: a hand-held point-of-care prototype. *Biosens. Bioelectron.* **2014**, *57*, 284−291.

(26) Wu, T.; Zhao, Y.; Zhao, Y. The roles of myeloid-derived suppressor cells in transplantation. *Expert Rev. Clin. Immunol.* **2014**, *10* (10), 1385−1394.

(27) Laffery, K. J.; Prowse, S. J.; Simeonovic, C. J.; Warren, H. S. Immunobiology of tissue transplantation: a return to the passenger leukocyte concept. *Annu. Rev. Immunol.* **1983**, *1* (1), 143−173.

(28) Benson, B.; Sorrentino, S.; Evans, J. S. Increase in serum FSH following unilateral ovariectomy in the rat. *Endocrinology* **1969**, *84* (2), 369−374.

(29) Kim, J.; Perez, A. S.; Claflin, J.; David, A.; Zhou, H.; Shikanov, A. Synthetic hydrogel supports the function and regeneration of artificial ovarian tissue in mice. *NPJ. Regen Med.* **2016**, *1*, 16010.

(30) Shikanov, A.; Zhang, Z.; Xu, M.; Smith, R. M.; Rajan, A.; Woodruff, T. K.; Shea, L. D. Fibrin encapsulation and vascular endothelial growth factor delivery promotes ovarian graft survival in mice. *Tissue Eng., Part A* **2011**, *17* (23−24), 3095−3104.

(31) Byers, S. L.; Wiles, M. V.; Dunn, S. L.; Taft, R. A. Mouse estrous cycle identification tool and images. *PLoS One* **2012**, *7* (4), No. e35538.

(32) Miller, B. H.; Takahashi, J. S. Central circadian control of female reproductive function. *Front. Endocrinol.* **2014**, *4*, 195.

(33) Staley, K.; Scharfman, H. A woman's prerogative. *Nat. Neurosci.* **2005**, *8* (6), 697−699.

(34) Scharfman, H. E.; MacLusky, N. J. Estrogen−growth factor interactions and their contributions to neurological disorders. *Headache* **2008**, *48* (s2), s77.

(35) David, A.; Day, J. R.; Cichon, A. L.; Lefferts, A.; Cascalho, M.; Shikanov, A. Restoring ovarian endocrine function with encapsulated ovarian allograft in immune competent mice. *Ann. Biomed. Eng.* **2017**, *45* (7), 1685−1696.

(36) Murr, S. M.; Geschwind, I.; Bradford, G. Plasma LH and FSH during different oestrous cycle conditions in mice. *Reproduction* **1973**, *32* (2), 221−230.

DOI: 10.1021/acssensors.8b00641
ACS Sens. 2018, 3, 2327−2334